IEEE Photonics Journal
An IEEE Photonics Society Publication

Open Access

Efficiency Enhancement of III-V Triple-Junction Solar Cell Using Nanostructured Bifunctional Coverglass With Enhanced Transmittance and Self-Cleaning Property

Volume 6, Number 3, June 2014

Chan Il Yeo
Eun Kyu Kang
Soo Kyung Lee
Young Min Song
Yong Tak Lee

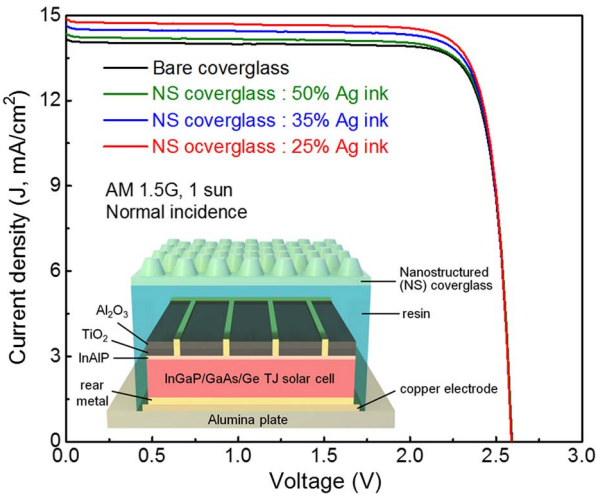

DOI: 10.1109/JPHOT.2014.2319100
1943-0655

Efficiency Enhancement of III-V Triple-Junction Solar Cell Using Nanostructured Bifunctional Coverglass With Enhanced Transmittance and Self-Cleaning Property

Chan Il Yeo,[1] Eun Kyu Kang,[1] Soo Kyung Lee,[1] Young Min Song,[1,2] and Yong Tak Lee[1,3]

[1]School of Information and Communications, Gwangju Institute of Science and Technology, Gwangju 500-712, Korea
[2]Department of Electronics Engineering, Pusan National University, Busan 609-735, Korea
[3]Advanced Photonics Research Institute, Gwangju Institute of Science and Technology, Gwangju 500-712, Korea

DOI: 10.1109/JPHOT.2014.2319100

Manuscript received March 5, 2014; revised April 9, 2014; accepted April 11, 2014. Date of publication April 22, 2014; date of current version May 7, 2014. This work was supported by the National Research Foundation of Korea (NRF) Grant funded by the Korean Government (MEST) under Grant 2011-0017606. Corresponding author: Y. T. Lee (e-mail: ytlee@gist.ac.kr).

Abstract: We present bifunctional nanostructured (NS) coverglasses with enhanced transmittance and self-cleaning function for improving the efficiency of a photovoltaic (PV) module with an InGaP/GaAs/Ge triple-junction solar cell. Prior to the fabrication of NS coverglasses, theoretical investigations were carried out using a rigorous coupled-wave analysis method to determine the desirable glass nanostructures that can effectively enhance the light absorption of the PV module. The transmission properties of the fabricated NS coverglasses with different glass nanostructures were systematically analyzed by considering the absorption spectrum of three subcells of the solar cell in order to find the most effective NS coverglass for enhancing the photocurrent of the PV module and thereby improving the conversion efficiency. The PV module with the most effective NS coverglass showed 4.2% enhanced short-circuit current density and 4.3% enhanced efficiency compared with the PV module with a bare coverglass measured under one sun of the air mass 1.5 global, showing the necessity of integrating a finely designed NS coverglass to effectively improve the efficiency of various PV systems with multijunction solar cells.

Index Terms: Nanostructured coverglass, III-V triple-junction solar cell, self-cleaning, rigorous coupled-wave analysis (RCWA) method.

1. Introduction

Photovoltaic (PV) systems with III-V compound semiconductor based multi-junction (MJ) solar cells are, due to their high conversion efficiency and strong durability, a promising form of renewable energy source to solve global-warming and energy shortage issues that our society faces [1]–[3]. In practice, PV systems are installed outdoors and face harsh weather conditions. Hence, a cover material is necessary to protect the solar cells from external shock, heat, ultra-violet (UV) irradiation, and corrosive acidic rain [4]. Glass has been widely used as a cover material of the PV systems due

to its beneficial properties such as high transmittance and resistance against weathering and UV radiation [5]. However, approximately 4% of Fresnel reflection loss at the sun-facing side of glass, which originate from the refractive index difference between air $(n_{air} = 1)$ and glass $(n_{glass} \sim 1.5)$, leads to less light being transmitted into the solar cell, thereby causing efficiency deterioration of the PV systems [5], [6]. Thus, surface antireflection is required to suppress the unwanted reflection loss at the air/glass interface for enhancing the transmission of sunlight into the solar cells and thereby improving the efficiency of the PV systems. The transmittance of coverglass for PV systems with MJ solar cells, in particular, should be enhanced by considering the absorption spectrum of each subcell. This is because the net photocurrent of MJ solar cell is limited by the subcell with the lowest photocurrent among series connected subcells [7]–[9]. Any enhancement in the light absorption of the subcell having the lowest photocurrent would therefore result in an increase in the net photocurrent and minimize the photocurrent difference between different subcells, which in turn would lead to an increase in the overall efficiency of PV systems with MJ solar cells. Self-cleaning function is also required to prevent the accumulation of surface contaminants on the coverglass and thereby maintaining the efficiency of the PV systems. It has been reported that the surface contaminants accumulated on the coverglass can block the transmission of sunlight into the solar cell resulting in a decline in the net efficiency of PV systems by 32%–40% within the first eight months of installation [10]–[13]. To satisfy both the requirements, surface relief nanostructures having excellent antireflection properties over a broad wavelength ranges and wide incident angles as well as with self-cleaning functionality are a promising candidate [4], [7], [11]–[17].

Herein, nanostructured (NS) coverglasses with enhanced transmittance and self-cleaning function were readily fabricated using spin-coating silver (Ag) ink, which can produce nano-scale etch mask through a simple, fast, and cost-effective method without any complicated equipments [15], and subsequent reactive ion etch (RIE) process in order to improve the conversion efficiency of PV modules with InGaP/GaAs/Ge triple-junction (TJ) solar cell. Prior to fabrication of NS glasses, theoretical calculation was carried out using a rigorous coupled-wave analysis (RCWA) method to determine the desirable period of glass nanostructure, which is a key parameter to achieve high transmittance throughout the entire solar spectrum, because the transmittance spectrum of NS glass is strongly correlated with their period [6], [16], [17]. The optical and wetting properties of NS coverglasses were systematically analyzed and the conversion efficiency of the PV modules with NS coverglasses was investigated.

2. Simulation and Experimental Details

2.1. Simulation of PV Modules With Various Coverglasses

The period of the glass nanostructure is crucial to achieve high transparency over a broad wavelength range because the transmittance of NS glass rapidly decreases as the period increases beyond the incident wavelength of light [6], [17]. Thus, based on theoretical calculations, it is essential to determine the desirable period of glass nanostructure prior to fabrication of NS coverglasses for enhancing the light absorption of the PV module over the entire absorption wavelength range of the TJ solar cell consisting of 0.7 μm-thick InGaP top cell, 3.65 μm-thick GaAs middle cell, and 150 μm-thick Ge bottom cell. Fig. 1(a) shows the calculated absorption of the PV modules with various coverglasses using RCWA method [18]. The absorption was obtained by subtracting the calculated reflectance (%) and transmittance (%) from 100%. The schematic illustration of a PV module with NS coverglass used in this calculation is presented in Fig. 1(b). In this calculation, hexagonally symmetric glass nanostructure having a truncated cone-shape with a height of 100 nm, a bottom diameter-to-period (BtoP) ratio of 0.9, and a top diameter-to-period (TtoP) ratio of 0.5 was assumed for simplifying the calculation. It was also assumed that the light absorption by the thin AlGaAs/InGaP and GaAs/GaAs tunnel diodes that interconnects the InGaP and GaAs subcells and GaAs and Ge subcells, respectively, is negligible. As an encapsulation material, silicon resin $(n_{resin} \sim 1.53)$ was used. A double layer antireflection coating consisting of 58 nm-thick TiO_2 $(n_{TiO_2} \sim 2.60)$ and 50 nm-thick Al_2O_3 $(n_{Al_2O_3} \sim 1.77)$ was employed on the top layer of the

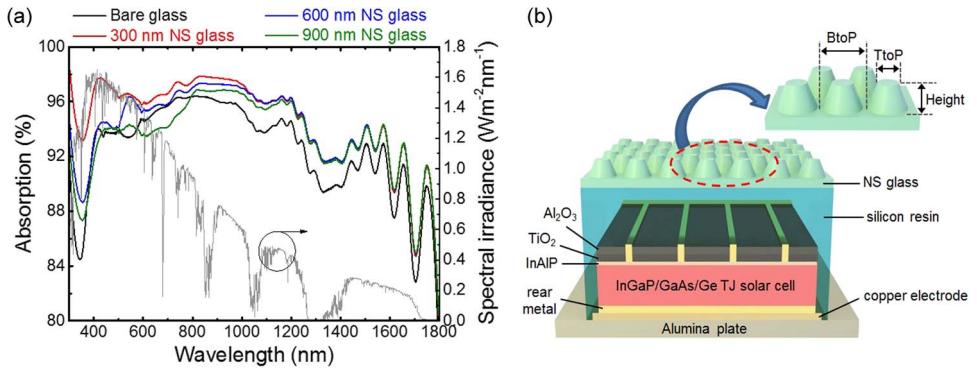

Fig. 1. Calculated absorption of PV modules with InGaP/GaAs/Ge TJ solar cell and various coverglasses. The height, BtoP ratio, and TtoP ratio of NS coverglass were fixed at 100 nm, 0.9, and 0.5, respectively. (b) The schematic illustration of a PV module with InGaP/GaAs/Ge TJ solar cell and NS coverglass.

TABLE 1

Calculated SWA of the PV modules with InGaP/GaAs/Ge TJ solar cell and coverglasses having different periods

Wavelength (nm)	Bare glass (%)	NS glass (%)		
		Period : 300 nm	Period : 600 nm	Period : 900 nm
300-660	93.38	96.37	94.52	93.29
660-870	96.09	97.21	96.59	95.41
870-1800	93.23	95.04	94.98	94.68

solar cell (i.e., InAlP window layer) [19]. As can be seen from Fig. 1(a), the PV modules with NS coverglass show higher light absorption than the one with bare coverglass in general. This is due to the enhanced light transmittance into the solar cell by integrating antireflective nanostructures on the surface of coverglass. As the period of glass nanostructure decreases, light absorption of the PV module increases, particularly in the short wavelength region. This can be attributed to the reduced surface reflection on the NS coverglass with decreasing period of nanostructure because the high-order (> zero-order) diffraction losses in nanostructure were suppressed as the period of nanostructures became smaller than the incident wavelength of light [6]. The calculation result shown in Fig. 1(a) strongly suggests that NS coverglass having a period of 300 nm or shorter would be the most effective one in absorbing photons in the shorter wavelength region and simultaneously over a broad wavelength range.

To investigate the effective light absorption of the PV module by considering solar spectrum and the absorption spectrum of each subcell of the TJ solar cell, we calculated the solar-weighted absorption (SWA) by dividing the wavelength range according to the dominant absorption wavelength range of each subcell (i.e., 300–660 nm, 660–870 nm, and 870–1800 nm for InGaP, GaAs, and Ge subcell, respectively). The SWA was calculated using the equation:

$$\mathrm{SWA} = \frac{\int F(\lambda) A(\lambda)\, d\lambda}{\int F(\lambda)\, d\lambda} \tag{1}$$

where $F(\lambda)$ is the photon flux rate in the air mass 1.5 global (AM 1.5G) spectrum and $A(\lambda)$ is the calculated absorption [20]. The calculated SWAs of various PV modules with bare coverglass and NS coverglasses are presented in Table 1. Among the various PV modules, the PV module with NS coverglass having a period of 300 nm exhibited much enhanced SWA for both the absorption

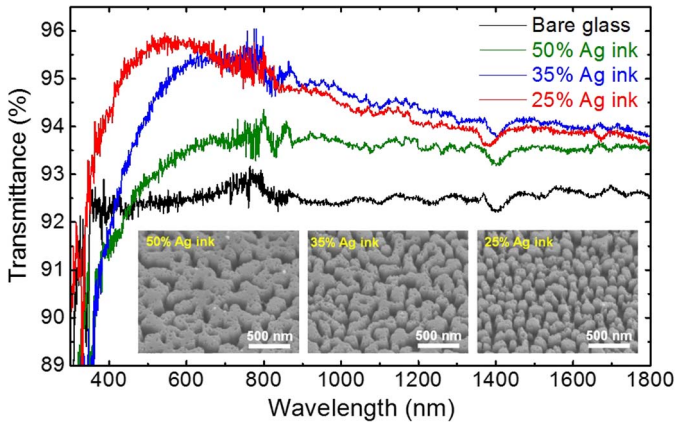

Fig. 2. Measured hemispherical transmittance spectra of the fabricated NS glasses using Ag ink ratios of 50%, 35%, and 25%. Insets show the fabricated glass nanostructures.

spectrum of InGaP and GaAs subcells, which generate much lower photocurrent compared to that of Ge subcell. It also exhibited the smallest SWA difference ($< 1\%$) between the absorption spectrum of InGaP and GaAs subcells, thereby minimizing the photocurrent mismatch between them. Therefore, the NS coverglass with a period less than 300 nm is highly desirable for improving the efficiency of the PV module with the TJ solar cell. This result also highlights the importance of integrating finely designed NS cover materials for effectively improving the efficiency of PV modules with various MJ solar cells.

2.2. Fabrication of NS Coverglasses

In this study, Ag etch masks formed using solvent-based spin-coating Ag ink and subsequent RIE process were used to fabricate NS glasses. To fabricate NS glass with desirable period, the Ag ink ratio in a mixed solution of isopropanol and Ag ink was carefully adjusted (i.e., Ag ink ratios of 50%, 35%, and 25%). The ink was spin-coated on a single-side of borosilicate glass (BoroFloat 33, Schott, USA) substrate, and then sintered on a hotplate at 200 °C for 5 min to form nano-scale Ag etch masks. It is worth noting that the temperature and time to produce Ag masks on glass substrate were much lower and shorter, respectively, than previously reported technique in which the nano-scale metal masks were formed through the thermal dewetting of evaporated thin metal film [11], [12], [16], [17]. This means that the fabrication cost and productivity of glass nanostructures can be reduced and enhanced, respectively, by using the spin-coating Ag ink. Further details regarding the Ag ink and the experimental procedure can be found in the literature [15]. RIE process was carried out at 75 W radio-frequency power and 20 mTorr process pressure for 9 min in a CF_4/O_2 plasma ambient. After the RIE process, the samples were soaked in a diluted mixture of potassium iodide and iodine etchant at room temperature to completely remove the residual Ag masks for 5 s. Finally, the samples were rinsed with deionized water and dried with nitrogen jet.

3. Results and Discussion

Fig. 2 shows the measured hemispherical transmittance spectra of the NS glasses fabricated using different Ag ink ratios of 50%, 35%, and 25%. The insets show 45°-tilted-view field-emission scanning electron microscope (FE-SEM, S-4700, Hitachi, Japan) images of the fabricated NS glasses corresponding to the ink ratios. The fabricated glass nanostructures showed an average height of 186 ± 7 nm. We estimated the average distance between the adjacent glass nanostructures (i.e., quasi-period) using a free-ware image processing program (ImageJ 1.42q, NIH). The glass nanostructures fabricated using an Ag ink ratio of 25% showed a desirable quasi-period of 231 ± 16 nm. The hemispherical transmittance spectra were measured using a UV-Vis-NIR spectrophotometer (Cary 500, Varian, USA) with an integrating sphere kept at near-normal incident angle of 8°. The

TABLE 2
Calculated SWT of bare glass and NS glasses produced using different Ag ink ratios

Wavelength (nm)	Bare glass (%)	NS glass (%)		
		50% Ag ink	35% Ag ink	25% Ag ink
300-660	92.35	92.68	93.91	95.24
660-870	92.69	93.75	95.28	95.18
870-1800	92.50	93.26	94.43	94.26
300-1800	92.48	93.24	94.43	94.87

measured transmittance of bare glass is also shown as a reference. The overall transmittance of the NS glasses was higher than the bare glass. However, the NS glasses fabricated using Ag ink ratios of 35% and 50% showed lower transmittance in the wavelength range shorter than $\sim$420 nm and $\sim$470 nm, respectively, compared to the bare glass. It is also seen that transmittance edge shifts toward longer wavelength with increasing Ag ink ratio due to the increased quasi-period of the fabricated glass nanostructures [6], [17]. It is noteworthy that the NS glass fabricated with an Ag ink ratio of 25% which had a quasi-period less than 300 nm was the most effective one in enhancing the light transmittance, particularly at shorter wavelength region.

We also investigated the transmittance of various glasses by calculating the solar-weighted transmittance (SWT) using the following equation:

$$\text{SWT} = \frac{\int F(\lambda) T(\lambda)\, d\lambda}{\int F(\lambda)\, d\lambda} \tag{2}$$

where $T(\lambda)$ is the measured transmittance. The calculated SWTs of the bare glass and that of NS glasses are presented in Table 2. From the calculated SWT, we convinced that the NS glass fabricated using 25% Ag ink ratio is the most desirable coverglass for the PV module with InGaP/GaAs/Ge TJ solar cell because it displayed an SWT of $>$ 95% in both the absorption spectrum of InGaP and GaAs subcells. From this result, we verified the importance of the period of glass nanostructure on the light transmission properties into the solar cell.

The effect of NS coverglasses on the performance of the PV modules was investigated by mounting the NS coverglasses on an InGaP/GaAs/Ge TJ solar cell with a TiO_2/Al_2O_3 double layer antireflection coating and an active area of 0.3025 cm^2. The coverglass was mounted by surrounding the solar cell by a silicon resin. Fig. 3 shows the measured current density-voltage (J-V) curves of the PV modules with various NS coverglasses. The insets of Fig. 3 show the photographs of the PV modules with bare coverglass (left) and NS coverglass (right) fabricated using 25% Ag ink. The TJ solar cell under the bare coverglass is less visible due to the surface reflection at the bare coverglass, whereas the one under the NS coverglass is clearly seen due to reduced surface reflection. The J-V characteristics were measured using a solar simulator (Sol3A, Oriel, USA) under one-sun of AM 1.5G at room temperature.

The performance characteristics of the PV modules with various coverglasses are summarized in Table 3. The number inside each parenthesis is the measured value before mounting the coverglass. It is important to note that the measured short-circuit current density (J_{sc}) was enhanced by employing NS coverglasses compared to the one with bare coverglass. The largest enhancement of J_{sc} (4.2% higher compared to the one with bare coverglass) was shown by the NS coverglass fabricated using 25% Ag ink ratio because it exhibited the most effective transmittance in both the absorption spectrum of InGaP and GaAs subcells. From additional calculations with parameters extracted from experiments, it is confirmed that the enhanced J_{sc} of the solar cell with a NS coverglass fabricated using 25% Ag ink ratio is predominantly due to the 4.4% and 3.3% enhanced SWA in the absorption spectrum of InGaP and GaAs subcell, respectively. Meanwhile, the open

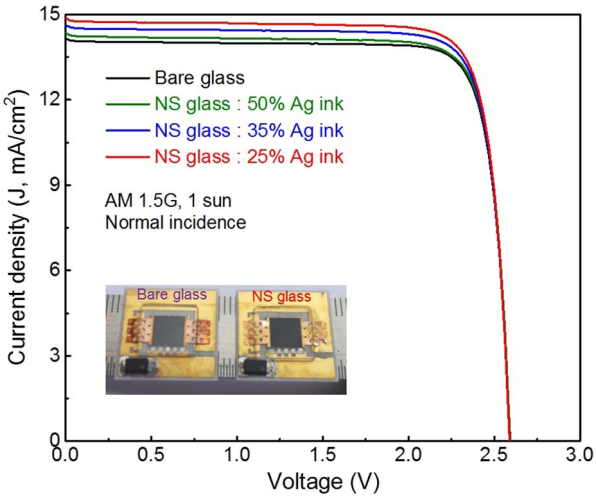

Fig. 3. J-V curves of the PV modules with InGaP/GaAs/Ge TJ solar cell and various coverglasses. The insets show the photographs of the PV modules with bare coverglass and NS coverglass fabricated using 25% Ag ink ratio.

TABLE 3

Summarized characteristics of the PV modules with bare coverglass and NS coverglasses

PV module	V_{oc} (V)	J_{sc} (mA/cm^2)	FF (%)	Efficiency (%)
Bare glass	2.591 (2.581)	14.27 (14.05)	82.4 (82.3)	30.48 (30.01)
NS glass using 50% Ag ink	2.592 (2.582)	14.35 (14.05)	82.2 (82.2)	30.61 (30.02)
NS glass using 35% Ag ink	2.590 (2.581)	14.62 (14.05)	82.3 (82.2)	31.26 (30.00)
NS glass using 25% Ag ink	2.589 (2.580)	14.87 (14.07)	82.1 (82.2)	31.80 (30.03)

circuit voltage (V_{oc}) and the fill factor (FF) were nearly the same even after mounting the coverglasses, indicating no deterioration in electrical properties of the PV modules. The efficiency (η), therefore, was improved by 4.3% compared to that of with the bare coverglass. These results clearly suggest the requirement of finely designed NS coverglass to effectively improve the conversion efficiency of PV modules with various MJ solar cells.

Incident angle-dependent conversion efficiency is another important parameter used to determine the performance of PV module. A good PV module with solar cell should be able to generate high and stable solar electricity during the daytime irrespective of change in the sun's altitude as the day progress. Fig. 4(a) shows the measured incident angle-dependent efficiency and J_{sc} of the PV modules with bare coverglass and NS coverglass fabricated using 25% Ag ink. As the angle of incidence (AOI, θ_i) was increased from 20° to 70°, the efficiency of the PV modules with bare coverglass and NS coverglass decreased from 28.5% to 10.9% and 30.2% to 13.0%, respectively. The efficiency drop is mainly due to the decreased J_{sc} (13.34 to 5.39 mA/cm^2 and 14.16 to 6.42 mA/cm^2 for the PV module with bare coverglass and NS coverglass, respectively) with increase in AOI from 20° to 70°. Meanwhile, the decrease in J_{sc} can be ascribed to the decreased incident angle-dependent SWT with an increase in the AOI as shown in Fig. 4(b). It is notable that the PV module with NS coverglass showed higher efficiency compared to the one with bare coverglass in the entire AOI. Although incident angle-dependent V_{oc} and FF were slightly

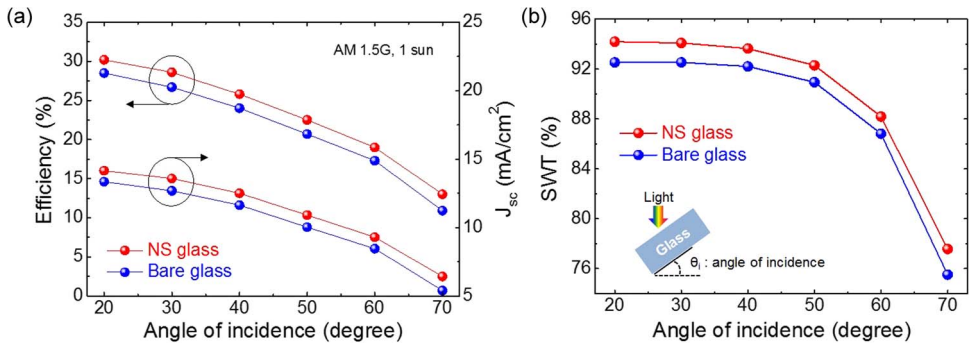

Fig. 4. (a) Incident angle-dependent efficiency and J_{sc} of the PV modules with bare coverglass and NS coverglass fabricated using 25% Ag ink. (b) Incident angle-dependent SWT of the bare glass and NS glass fabricated using 25% Ag ink.

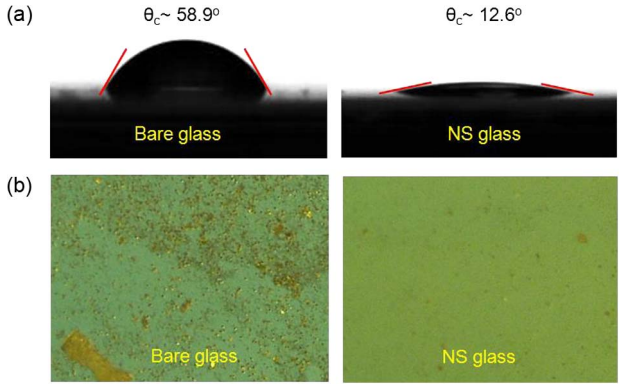

Fig. 5. (a) Water droplet on bare glass and NS glass with their corresponding contact angle. (b) Microscope images of bare glass and NS glass after exposed outdoors for 3 weeks.

decreased from 2.57 to 2.51 $\pm$ 0.004 V and 82.3 to 76.9 $\pm$ 0.3%, respectively, these changes did not significantly affect the incident angle-dependent efficiency.

In real environment, PV modules are installed outdoors and surface contaminants such as dust particles and sand are accumulated on the coverglass surface thereby causing degradation in the conversion efficiency by blocking the transmission of sunlight into solar cell [10]–[12]. Hence, self-cleaning functionality is highly required to clean the surface of the coverglass. Fig. 5(a) shows the photographs of water droplets on the surface of bare glass (left) and NS glass (right). To investigate the wetting properties of bare glass and NS glass, the contact angles (θ_c) of a water droplet was measured using a contact angle measurement system (Phoenix-300 Touch, SEO Co., Ltd., Republic of Korea). The NS glass exhibited improved hydrophilicity $(\theta_c \sim 12.6^\circ)$ compared to that of bare glass $(\theta_c \sim 58.9^\circ)$ due to enhanced surface roughness [16]. It is generally known that the hydrophobic surface has self-cleaning function (Lotus leaf's effect) as reported in literature [4], [13], [21]. Note that a hydrophilic surface also can provide self-cleaning function [11], [12], [21]. The flowing liquid film on the inclined hydrophilic surface can wash away the surface contaminants. The usefulness of this feature can be validated by an outdoor testing as shown in the microscope images of Fig. 5(b). The bare glass and NS glass tilted at 45° were exposed to outdoor for 3 weeks of which there were four rainy days. The NS glass shows a clean surface due to its self-cleaning function, whereas the bare glass shows a contaminated surface due to the accumulation of dust particles and sand. We therefore found that the NS coverglass can not only improve the efficiency of PV modules by enhancing light transmission into solar cell, but also can provides self-cleaning capability which can maintain the efficiency of PV modules for longer duration. In addition, the NS

covers are also effective in enhancing the performance of light emitting diodes by reducing unwanted reflections that occur at the interface between the outermost layer of LED and air [22]–[24].

4. Conclusion

We fabricated highly transparent NS coverglass using spin-coating Ag ink to improve the efficiency of PV module with InGaP/GaAs/Ge TJ solar cell. Theoretical calculation based on RCWA method was performed prior to fabrication in order to determine the desirable period of glass nanostructures for effectively improving the efficiency of the PV module. By adjusting the Ag ink ratio, various NS glasses having different quasi-period were fabricated. The NS coverglass fabricated using 25% Ag ink ratio which had a quasi-period less than 300 nm showed the most desirable light transmittance for enhancing the photocurrent of the TJ solar cells. Therefore, the PV module with NS coverglass fabricated using 25% Ag ink ratio showed the largest enhancement in J_{sc} and efficiency. The PV module with NS coverglass also showed a superior incident angle-dependent efficiency than the one with bare coverglass due to enhanced incident angle-dependent SWT of the NS coverglass. In addition, the NS coverglass demonstrated self-cleaning capability which helps to maintain the efficiency of PV module for longer duration. From these results, it was found that integrating finely designed NS cover material is absolutely necessary to effectively improve and maintain the efficiency of various PV systems with MJ solar cells.

Acknowledgment

The authors wish to thank S. Ravindran for technical comments and suggestions.

References

[1] J. A. Turner, "A realizable renewable energy future," *Science*, vol. 285, no. 5428, pp. 687–689, Jul. 1999.
[2] D. J. Friedman, "Progress and challenges for next-generation high-efficiency multijunction solar cells," *Current Opinion Solid State Mater. Sci.*, vol. 14, no. 6, pp. 131–138, Dec. 2010.
[3] M. A. Green, K. Emery, Y. Hishikawa, W. Warta, and E. D. Dunlop, "Solar cell efficiency tables (version 43)," *Progr. Photovoltaics*, vol. 22, no. 1, pp. 1–9, Jan. 2014.
[4] J.-H. Shin, K.-S. Han, and H. Lee, "Anti-reflection and hydrophobic characteristics of M-PDMS based moth-eye nano-patterns on protection glass of photovoltaic systems," *Progr. Photovoltaics*, vol. 19, no. 3, pp. 339–344, May 2011.
[5] J. Deubener, G. Helsch, A. Moiseev, and H. Bornhöft, "Glasses for solar energy conversion systems," *J. Eur. Ceram. Soc.*, vol. 29, no. 7, pp. 1203–1210, Apr. 2009.
[6] Y. M. Song, H. J. Choi, J. S. Yu, and Y. T. Lee, "Design of highly transparent glasses with broadband antireflective subwavelength structures," *Opt. Exp.*, vol. 18, no. 12, pp. 13 063–13 071, Jun. 2010.
[7] M.-Y. Chiu, C.-H. Chang, M.-A. Tsai, F.-Y. Chang, and P. Yu, "Improved optical transmission and current matching of a triple-junction solar cell utilizing sub-wavelength structures," *Opt. Exp.*, vol. 18, no. S3, pp. A308–A313, Sep. 2010.
[8] Y.-J. Lee *et al.,* "Current matching using CdSe quantum dots to enhance the power conversion efficiency of InGaP/GaAs/Ge tandem solar cells," *Opt. Exp.*, vol. 21, no. S6, pp. A953–A963, Nov. 2013.
[9] K. Nishioka *et al.,* "Evaluation of InGaP/InGaAs/Ge triple-junction solar cell and optimization of solar cells's structure focusing on series resistance for high-efficiency concentrator photovoltaic systems," *Sol. Energy Mater. Solar Cells*, vol. 90, no. 9, pp. 1308–1321, 2006.
[10] M. J. Adinoyi and S. A. M. Said, "Effect of dust accumulation on the power outputs of solar photovoltaic modules," *Renew. Energy*, vol. 60, pp. 633–636, Dec. 2013.
[11] J. Son *et al.,* "A practical superhydrophilic self cleaning and antireflective surface for outdoor photovoltaic applications," *Sol. Energy. Mater. Solar Cells*, vol. 98, pp. 46–51, Mar. 2012.
[12] L. K. Verma *et al.,* "Self-cleaning and antireflective packaging glass for solar modules," *Renew. Energy*, vol. 36, no. 9, pp. 2489–2493, Sep. 2011.
[13] J. Zhu, C.-M. Hsu, Z. Yu, S. Fan, and Y. Cui, "Nanodome solar cells with efficient light management and self-cleaning," *Nano Lett.*, vol. 10, no. 6, pp. 1979–1984, Jun. 2010.
[14] Y. M. Song, S. J. Jang, J. S. Yu, and Y. T. Lee, "Bioinspired parabola subwavelength structures for improved broadband antireflection," *Small*, vol. 6, no. 9, pp. 984–987, May 2010.
[15] C. I. Yeo, J. H. Kwon, S. J. Jang, and Y. T. Lee, "Antireflective disordered subwavelength structure on GaAs using spin-coated Ag ink mask," *Opt. Exp.*, vol. 20, no. 17, pp. 19 554–19 562, Aug. 2012.
[16] J. W. Leem, Y. Yeh, and J. S. Yu, "Enhanced transmittance and hydrophilicity of nanostructured glass substrates with antireflective properties using disordered gold nanopatterns," *Opt. Exp.*, vol. 20, no. 4, pp. 4056–4066, Feb. 2012.
[17] G. C. Park, Y. M. Song, E. K. Kang, and Y. T. Lee, "Size-dependent optical behavior of disordered nanostructures on glass substrate," *Appl. Opt.*, vol. 51, no. 24, pp. 5890–5896, Aug. 2012.

[18] M. G. Moharam and T. K. Gaylord, "Rigorous coupled-wave analysis of planar-grating diffraction," *J. Opt. Soc. Amer.*, vol. 71, no. 7, pp. 811–818, Jul. 1981.
[19] M. Victoria, C. Domínguez, I. Antón, and G. Sala, "Antireflective coatings for multijunction solar cells wide-angle ray bundles," *Opt. Exp.*, vol. 20, no. 7, pp. 8136–8147, Mar. 2012.
[20] [Online]. Available: http://rredc.nrel.gov/solar/spectra/am1.5/
[21] R. Blossey, "Self-cleaning surfaces—virtual realities," *Nat. Mater.*, vol. 2, no. 5, pp. 301–306, May 2013.
[22] W. H. Koo *et al.,* "Light extraction of organic light emitting diodes by defective hexagonal-close-packed array," *Adv. Funct. Mater.*, vol. 22, no. 16, pp. 3454–3459, Aug. 2012.
[23] P. Zhu, G. Liu, J. Zhang, and N. Tansu, "FDTD analysis on extraction efficiency of GaN light-emitting diodes with microsphere arrays," *J. Display Technol.*, vol. 9, no. 5, pp. 317–323, May 2013.
[24] E. K. Kang, Y. M. Song, S. J. Jang, C. I. Yeo, and Y. T. Lee, "Increased light extraction from GaN light-emitting diodes by SiN_x compound eyes," *IEEE Photon. Technol. Lett.*, vol. 25, no. 12, pp. 1118–1121, Jun. 2013.